

ON THE TRANSFER OF RESONANT-LINE RADIATION IN MESH SIMULATIONS

ARGYRO TASITSIMI¹*draft version; February 7, 2020*

ABSTRACT

The last decade has seen applications of Adaptive Mesh Refinement (AMR) methods for a wide range of problems from space physics to cosmology. With the advent of these methods, in which space is discretized into a mesh of many individual cubic elements, the contemporary analog of the extensively studied line radiative transfer (RT) in a semi-infinite slab is that of RT in a cube. In this study we provide an approximate solution of the RT equation, as well as analytic expressions for the probability distribution functions (pdfs) of the properties of photons emerging from a cube, and compare them with the corresponding slab problem. These pdfs can be used to perform fast resonant-line RT in optically thick AMR cells where, otherwise, it could take unrealistically long times to transfer even a handful of photons.

Subject headings: line: formation — radiative transfer — resonant

1. INTRODUCTION

The classic problem of resonant radiative transfer (RT) in a semi-infinite slab has been extensively studied in literature (e.g., Harrington 1973; Neufeld 1990). On the other hand, the last decade has seen applications of Adaptive Mesh Refinement (AMR) methods to problems as diverse as solar physics, supernovae and nucleosynthesis, interstellar medium physics, star formation, astrophysical jets, cosmology, etc. (for a summary see, e.g., Norman 2004). In mesh-based methods the continuous domain of interest is discretized into a grid of many individual cubic elements. With the advent of AMR codes, the contemporary analogue — at least in terms of usefulness and applicability range — of the extensively studied problem of resonant-line RT in a slab is the relatively unexplored problem of RT in a cube.

Understanding resonant RT in optically thick cubes is useful in particular because to perform RT in AMR simulations one must solve numerous cube RT problems, since each time a photon enters an AMR cell one has a new cube RT problem. Furthermore, as is the case, e.g., for Ly- α line RT in cosmological simulations of galaxy formation, the high resolution achieved with AMR codes (along with the cooling of the gas), leads to very high scattering optical depths (see Tasitsiomi 2005). To obtain results within realistic times, we need a very fast RT algorithm, faster than the standard direct Monte Carlo approach in which one follows the detailed scattering of photons in each one of the cells. A way to obtain this very fast algorithm is to study a priori the RT in cubes of various physical conditions. Using the results of such a study, we can avoid following the detailed photon scattering in each cell. Instead, we can immediately take the photon out of the cell treating thus the problem on a per cell rather than on a per scattering basis, thus accelerating the RT scheme considerably.

In this letter we discuss results on the resonant RT in a cube, and in comparison with resonant RT in a slab of similar physical conditions.

¹ Lyman Spitzer Fellow, Department of Astrophysical Sciences, Princeton University, Peyton Hall, Ivy Lane, Princeton, NJ 08544-1001; iro@astro.princeton.edu

2. DESCRIPTION OF THE PROBLEM AND DEFINITIONS

In what follows we assume slab and cube configurations for the scattering medium. The slab is semi-infinite, namely it is finite in one spatial dimension and infinite in the other two. The scattering medium is uniform in its properties and has a central source of center-of-line photons that scatter resonantly before escaping. Harrington (1973) has solved the slab RT equation in the limit of high optical depths and obtained a one parameter solution (also, see Neufeld 1990). The parameter is $\alpha\tau_0$, with $\alpha = \Delta\nu_L/2\Delta\nu_D$ and $\Delta\nu_L, \Delta\nu_D$ the line natural and thermal Doppler widths, respectively, and τ_0 the center-of-line optical depth from the center of the scattering medium to one of its edges. More specifically, τ_0 is defined so that the optical depth at frequency shift $x_f = (\nu - \nu_0)/\Delta\nu_D$ is $\tau_{x_f} = \tau_0\phi(x_f)$, with $\phi(x_f)$ the normalized line profile. The discussion that follows applies to optically thick media ($\alpha\tau_0 > 10^3$).

3. RESULTS

3.1. Emerging frequency distribution

3.1.1. Analytic solution for resonant RT in a cube

Following Harrington (1973), one can show that the RT equation we need to solve is

$$\nabla_{\vec{\tau}}^2 J(\vec{\tau}; \sigma) + \frac{\partial^2 J}{\partial \sigma^2} = -3\phi^2(x_f) \frac{j(\vec{\tau})}{4\pi} \quad (1)$$

where J is the zeroth moment of the intensity I , σ is defined through $\partial x_f / \partial \sigma = (3/2)^{1/2} \phi(x_f)$, τ is defined through $d\tau_{x_f} = \phi(x_f) d\tau$, and $j(\vec{\tau})$ is the emissivity. This equation is identical to the equation used previously for a semi-infinite slab (Unno 1955; Harrington 1973; Neufeld 1990) or a spherically symmetric distribution (e.g., Dijkstra et al. 2005). The only difference is that those previous cases were for one spatial dimension, hence $\nabla_{\vec{\tau}}^2$ consisted of only one term, whereas in the case of a cube it has contributions from all three dimensions, i.e. $\nabla_{\vec{\tau}}^2 = \partial^2 J / \partial \tau_x^2 + \partial^2 J / \partial \tau_y^2 + \partial^2 J / \partial \tau_z^2$.

To obtain an approximate solution for equation (1), we focus first on the solution of the corresponding homogeneous equation (Unno 1955). We assume that the solution is separable, namely that $J(\vec{\tau}, \sigma) = R(\vec{\tau})G(\sigma)$. Substituting in equation (1) and after some rearrangement we

get

$$\frac{\nabla_{\vec{\tau}}^2 R(\vec{\tau})}{R(\vec{\tau})} = -\frac{1}{G(\sigma)} \frac{\partial^2 G(\sigma)}{\partial \sigma^2} = -\lambda^2, \quad (2)$$

where we have performed a first separation with separation constant $-\lambda^2$. Assuming furthermore that $R(\vec{\tau}) = X(\tau_x)Y(\tau_y)Z(\tau_z)$, after performing additional separations we end up with equations of the form

$$\frac{1}{X} \frac{\partial^2 X}{\partial \tau_x^2} = -l^2 \quad (3)$$

and similarly for $Y(\tau_y), Z(\tau_z)$ with separation constants $-m^2$ and $-n^2$, respectively, and with $\lambda^2 = n^2 + l^2 + m^2$. The general solution for each one of these equations consists of both sine and cosine terms. Since we only consider central point sources, i.e. $j(\tau) = \delta(\tau_x)\delta(\tau_y)\delta(\tau_z)$, each one of the functions X, Y , and Z must be separately even. Thus, we set $X(\tau_x) = A \cos(l\tau_x)$, $Y(\tau_y) = B \cos(m\tau_y)$ and $Z(\tau_z) = C \cos(n\tau_z)$.

We calculate the constants A, B, C using boundary conditions that are generated assuming the Milne-Eddington approximation (see, e.g., p 322 of Eddington 1926). In fact, we adapt the usual two stream approximation to the cube problem. We take into account all 3 spatial directions and treat them equivalently. That is, we use an eight-stream approximation, which nevertheless, leads to the same conditions as the two stream approximation. Now, however, these conditions refer separately to each one of the three independent directions. Thus, we get $F_x(\pm\tau_0, \tau_y, \tau_z; \sigma) = 2J(\pm\tau_0, \tau_y, \tau_z; \sigma)$, with $F_i = \int I n_i d\Omega / \pi$ the flux components. This condition yields

$$\begin{aligned} J(\pm\tau_0, \tau_y, \tau_z; \sigma) &= \pm F(\pm\tau_0, \tau_y, \tau_z; \sigma) / 2 \\ &= \pm 2H(\pm\tau_0, \tau_y, \tau_z; \sigma) = \mp \frac{2}{3\phi(x_f)} \frac{\partial J}{\partial \tau_x} \Big|_{\tau_x=\pm\tau_0} \end{aligned} \quad (4)$$

with H the first moment of I (differing from the flux F by a factor of 1/4), and where, in order to obtain the last equality, we used the other Milne-Eddington condition, $J = 3Tr(K)$, with K the second moment of I with respect to \vec{n} , combined with that $\nabla_{\vec{\tau}} K / \phi(x_f) = H$. Using equation (4) we get for l_α the condition (also see, e.g., Neufeld 1990)

$$l_\alpha \tau_0 \simeq \pi(\alpha - 1/2) \left\{ 1 - \frac{2}{3\phi\tau_0} + O\left[\frac{1}{(\phi\tau_0)^2}\right] \right\}, \quad (5)$$

as well as similar conditions for m_β and n_γ .

Normalizing the cosine solutions in $[-\tau_0, \tau_0]$ in each direction separately, the solution to the homogeneous equation RT equation takes the form

$$\begin{aligned} J(\tau_x, \tau_y, \tau_z; \sigma) &= \sum_{\alpha, \beta, \gamma=1}^{\infty} \cos(l_\alpha \tau_x) \cos(m_\beta \tau_y) \cos(n_\gamma \tau_z) \\ &\quad \times G_{\alpha\beta\gamma}(\sigma) / \tau_0^{3/2}. \end{aligned} \quad (6)$$

Substituting this in equation (1), and after multiplying by $\cos(l_\alpha \tau_x) \cos(m_\beta \tau_y) \cos(n_\gamma \tau_z) / \tau_0^{3/2}$, and integrating over volume we get

$$-\lambda_{\alpha\beta\gamma}^2 G_{\alpha\beta\gamma} + \frac{\partial^2 G_{\alpha\beta\gamma}}{\partial \sigma^2} = -\frac{\sqrt{6}}{4\pi\tau_0^{3/2}} \delta(\sigma) Q_{\alpha\beta\gamma} \quad (7)$$

with

$$Q_{\alpha\beta\gamma} = \int_{-\tau_0}^{\tau_0} \int_{-\tau_0}^{\tau_0} \int_{-\tau_0}^{\tau_0} j(\vec{\tau}) \cos(l_\alpha \tau_x) \cos(m_\beta \tau_y) \cos(n_\gamma \tau_z) d\tau_x d\tau_y d\tau_z. \quad (8)$$

For a source of unit strength at the center of the cube we have $j(\vec{\tau}) = \delta(\tau_x)\delta(\tau_y)\delta(\tau_z)$, and thus $Q_{\alpha\beta\gamma} = 1$. In equation (7) we set $3\phi(x_f)^2 = \sqrt{6}\delta(\sigma)$ (see, Harrington 1973).

Away from $\sigma = 0$ equation (7) is homogeneous. Imposing the boundary condition $J(\vec{\tau}, \pm\infty) = 0$ that reflects the fact that we do not expect photons with infinite frequency shifts (thus, $G_{\alpha\beta\gamma}$ must go to zero for high – positive or negative – σ values) we get

$$G_{\alpha\beta\gamma}(\sigma) = D e^{-\lambda_{\alpha\beta\gamma} |\sigma|}. \quad (9)$$

We obtain the value of the constant D exactly as in Harrington (1973). Plugging all these in equation (6) and, since we are interested in the overall spectrum of radiation emerging from one side of the cube, say along the z axis, after integrating over τ_x, τ_y and setting $\tau_z = \tau_0$ we get

$$\begin{aligned} J(\tau_0, \sigma) &= \sum_{\alpha, \beta, \gamma=1}^{\infty} \frac{\sin(l_\alpha \tau_0)}{l_\alpha \tau_0} \frac{\sin(m_\beta \tau_0)}{m_\beta \tau_0} \cos(n_\gamma \tau_0) \\ &\quad \times \frac{\sqrt{6}}{2\pi} \frac{e^{-\sqrt{(l_\alpha \tau_0)^2 + (m_\beta \tau_0)^2 + (n_\gamma \tau_0)^2} |\sigma| / \tau_0}}{\sqrt{(l_\alpha \tau_0)^2 + (m_\beta \tau_0)^2 + (n_\gamma \tau_0)^2}}. \end{aligned} \quad (10)$$

At this last step we also substituted $\lambda_{\alpha\beta\gamma}^2$ with $l_\alpha^2 + m_\beta^2 + n_\gamma^2$. For a comparison of the spectrum emerging from one side of a cube to that emerging from one of the two 'sides' of a slab we must multiply our cube solution by a factor of 3 so that both solutions have the same normalization. This is so because, for the same central source, we expect 1/6 of the photons to emerge from a certain cube side and 1/2 of the photons to emerge from a certain slab 'side'.

Each individual series term for both the cube and the slab solution (given in Harrington 1973) depends only on $\alpha\tau_0$. This becomes obvious when one takes into account the definition of σ and the approximation for $\phi(x_f) \simeq \alpha/\pi x_f^2$ in the wings, as well as condition (5). The slab solution is an alternate series and can be written in closed form. The cube solution cannot be written in closed form, but, using equations (4) and (5) we see that $\sin(l_\alpha \tau_0) \simeq (-1)^{\alpha-1}$ and $\cos(n_\gamma \tau_0) = 2n_\gamma/3\phi(x_f)(-1)^{\gamma-1}$. Thus, the $\sin(l_\alpha \tau_0) \sin(m_\beta \tau_0) \cos(n_\gamma \tau_0)$ term in equation (10) can be written as $-(-1)^{\alpha+\beta+\gamma}$, indicating that the cube series may also be alternating. Writing this three-sum series as one sum, i.e., $\sum_{i=1}^{\infty} c_i$, we find that indeed the cube series is alternating as well. Some of the first finite sums of the alternating series for a $\alpha\tau_0 = 2 \times 10^4$ cube and slab are shown at the top two panels, and the left bottom panel of Figure 1, respectively. In the case of the cube the infinite number of terms result (solid histograms) is obtained by the Monte Carlo method described in detail in Tasitsiomi (2005), whereas for the slab we use the closed form slab analytical solution of Harrington (1973).

The cube series solution will be of some practical value, only if a few first terms contribute significantly to the sum. The exponential decay in $|\sigma|$ indicates that the terms should die off for 'high' α, β and γ values—with the exact values where this happens dependent on the frequency (or σ) one calculates the spectrum at. The logarithm of the absolute ratio of the series terms, c_i , in units of the first term, c_1 , for 3 different values of the frequency shift is shown in the bottom right panel of Figure 1. As before, $\alpha\tau_0 = 2 \times 10^4$, but we find that these 'convergence

curves' remain identical for all cube $\alpha\tau_0$ at the extremely optically thick regime. The dashed-dotted line is the 'convergence curve' for a slab for frequency shift equal to the shift where the emergent spectrum is known to have a maximum ($\sim 0.9(\alpha\tau_0)^{1/3}$; Harrington 1973). Away from this maximum, the slab convergence curves look identical to those of the cube (dotted and dashed lines). Clearly, the rate of convergence depends on the frequency the spectrum is calculated at. Given that the series is alternating, with the absolute value of the terms decreasing monotonically (for most σ values), the absolute error we make by truncating the series at the i th term is less or equal to the $i+1$ term. From the plot, this means that if we only keep the first term, the actual infinite series limit S will be $\simeq (1\pm 10^{-4})S_1$ for $x_f = 39$ and $\simeq (1\pm 0.3)S_1$ for $x = x_{max}$, with S_i the i th partial sum. We can achieve a 3% accuracy at the peak if we go to $i = 4$ (i.e., $|S - S_4|/S \leq 0.03$), whereas for better accuracy we have to exceed $i = 30$. Convergence becomes extremely slow at values close to the resonance, e.g., $x = 2$. Furthermore, we find that the up to $i = 30$ terms for $x = 2$ do not decrease monotonically in the case of the cube – they do decrease for the slab but extremely slowly.

The usefulness of the slab series solution derived here depends on the application in mind. For example, when studying Ly- α emitters at very high redshifts, it is expected that the blue frequencies will be absorbed anyway because of hydrogen intervening between the emitter and the observer, and the red wavelengths near the resonance will also be absorbed by the red damping wing. In this case, the poor convergence at frequencies near resonance (and, more generally, over the $|x| \leq x_{max}$ range) may not be a problem. Clearly, one must decide on the usefulness of the series solution based on the specifics of the application.

3.1.2. Approximate cube spectrum in closed form

Based on the similarities between the cube and the slab spectra, one might think that the spectrum emerging from one side of a cube may be well described by the slab closed form solution, but for a different, smaller $\alpha\tau_0$ than the actual $\alpha\tau_0$ of the cube. Because, for example, when observing the spectrum emerging from a cube along the z -direction we lose all photons that in the case of a slab would wander, scatter many times along the infinite dimensions until they finally escape from the z -plane. In the case of the cube these photons do not contribute to the spectrum we observe from the z -direction because they have already exited the cube along directions other than z . This argument has been already used in Tasitsiomi (2005), where the slab solution was used to describe the spectrum for a cube by plugging in the slab solution an $\alpha\tau_0$ equal to $2/3$ the actual cube $\alpha\tau_0$. This value was motivated by comparing the mean number of scatterings, N_{sc} , for photon escape in cubes and slabs. Since N_{sc} scales linearly with τ_0 for extremely optically thick media (Adams 1972), by comparing N_{sc} for cubes and slabs one can guess a correct effective τ_0 (and thus $\alpha\tau_0$). For the purposes of this previous study, this effective thickness gave good agreement with simulated spectra for a wide range of physical conditions.

Attempting a more detailed treatment, we fit cube spec-

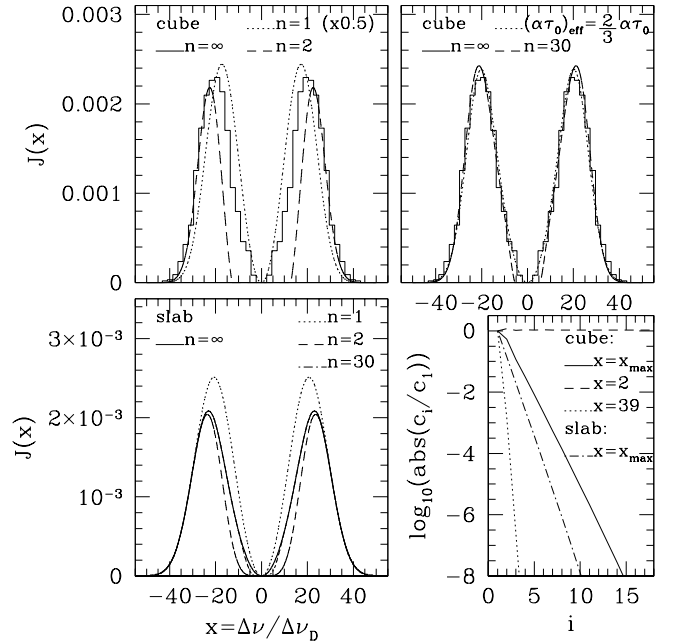


FIG. 1.— *Top left panel:* Cube emergent spectrum obtained via Monte Carlo RT simulation (solid histogram— $n = \infty$), and approximate analytical spectra using the one or two first terms of the sum given by equation (10) (dotted and dashed line, respectively). The $n = 1$ spectrum is multiplied by 0.5 to fit within the same y-axis range as the other spectra. *Top right panel:* Same as in left panel but for $n = 30$ terms (dashed line). Also shown is the spectrum obtained using the slab solution for a smaller, effective $\alpha\tau_0$ (dotted line). *Bottom left panel:* Slab emergent spectra using for the slab infinite number of terms (solid line—obtained using the closed form solution), one term (dotted line), two terms (dashed line), and the first thirty terms (dot-dashed line). *Bottom right panel:* Logarithm of the absolute value of the i th term of the sum representing the spectrum for a cube/slab, in units of the first term c_1 . Results are shown for the spectrum estimated at different frequency shifts, x . For most x values we show results only for the cube, since cube and slab terms exhibit the same convergence behavior, except near the frequencies where they attain their maximum intensity (x_{max}). All results are for $\alpha\tau_0 = 2 \times 10^4$. See text for details.

tra with the slab solution for the fraction f of $\alpha\tau_0$ that must be used in this solution to get the best fit. We find that f varies in the $0.66 - 0.77$ range for $\alpha\tau_0$ values in the $2 \times 10^3 - 10^8$ range. We find no trend of f with $\alpha\tau_0$. Within errors, one can use a constant fraction in the above f -range regardless of $\alpha\tau_0$ since we find that we cannot distinguish between the fits obtained when $2/3$ or the exact f value are used. An example of a fit of the cube spectrum using the slab solution and $f = 2/3$ is shown at the top, right panel of Figure 1 (the best fit f -value for this example is 0.72). Furthermore, in terms of the spectrum shape (e.g., maximum location and intensity), the above range of f values lead to spectra indistinguishable by currently existing instruments.

3.2. Distribution of exiting direction and point

Referring to μ , the cosine of the angle with which the photon is exiting, measured with respect to the normal to the exiting surface, we show its cumulative probability distribution function (cpdf) at the top panel of Figure 2. We find that this cpdf is the same for a slab or a cube,

and clearly deviates from isotropy (dashed line). We verify the findings of other studies that in optically thick media photons tend to exit in directions perpendicular to the exiting surface (see, e.g., Phillips & Meszaros 1986; Ahn et al. 2002).

In cases of very optically thick media, the emerging radiation directionality approaches the Thomson scattered radiation emergent from a Thomson-thick electron medium. Phillips & Meszaros (1986) found that for a Thomson-thick medium $I(\mu)/I(0) = (1 + 2\mu)/3$. Since the number

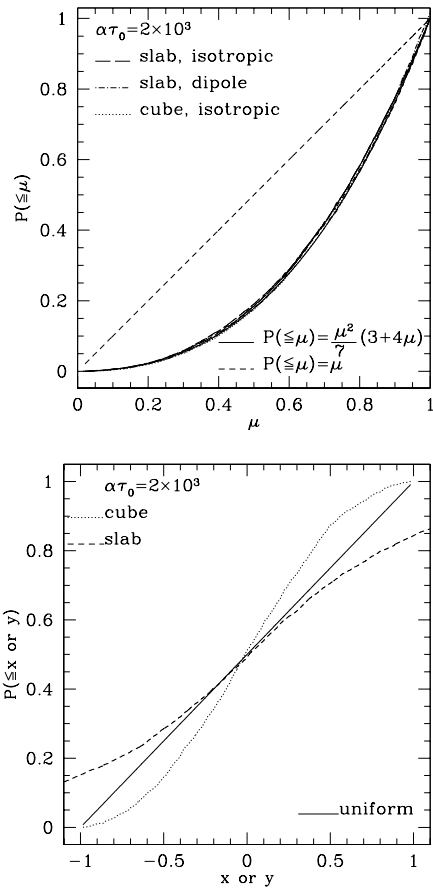


FIG. 2.— *Top panel:* Cumulative probability distribution function of the cosine of the angle the photon exiting direction forms with the normal to the exiting surface (μ). Results are shown for a semi-infinite slab or a cube (*long-dashed* and *short-dashed*, respectively), as well as for an isotropic or dipole scattering phase function (*long-dashed* and *dot-dashed* line, respectively). With the *solid line* we show the directionality of radiation emerging from a Thomson-thick electron medium. All these distributions are indistinguishable. Also shown is the case where photons exit the slab (or cube) isotropically (*dashed* line). *Bottom panel:* Cumulative probability distribution function of exit points of radiation emerging from a slab (*dashed* line) and a cube (*dotted* line) of the same $\alpha\tau_0$. The photons are assumed to emerge along the z direction, hence the distribution refers to either the x or y coordinate, in units of the size of the cube (or the finite dimension of the slab).

of photons emerging at μ is $\propto I(\mu)\mu d\mu$, we get

$$P(\leq \mu) = \frac{\int_0^\mu (1 + 2\mu)\mu d\mu}{\int_0^1 (1 + 2\mu)\mu d\mu} = \frac{\mu^2}{7}(3 + 4\mu). \quad (11)$$

This dependence is shown in Figure 2 with the solid line. It is an excellent description of the directionality of the

spectrum and hence equation (11) can be used to determine the photon exiting direction. It has been suggested by some authors (Ahn et al. 2002) that the fact that in optically thick media RT occurs mostly via wing photons with the latter being described by a dipole phase function (Stenflo 1980), and the fact that Thomson scattering is also described by a dipole scattering phase function explain why the resulting μ cpdfs are similar. However, we find the same cpdf if we use either an isotropic or a dipole phase distribution. For such optical thicknesses the details of the exact phase function do not matter, at least not with respect to the exiting angle cpdf. Regardless of scattering phase function, in such media photons tend to escape along the normal to the exiting surface where the opacity is smaller. The results shown are for $\alpha\tau_0 = 2 \times 10^3$, but similar distributions are obtained for thicker media.

In the case of the slab the azimuthal angle ϕ is distributed uniformly in $[0, 2\pi]$. In the case of the cube there are small deviations from uniformity. This is expected since the previous distribution for μ is found to be valid for *all* sides of the cube. In the simplest case where we observe along the z -axis (in which case the spherical coordinate ϕ angle is the actual azimuthal angle we refer to), all direction cosines – $\cos\theta$ and $\sin\theta\cos\phi$ and $\sin\theta\sin\phi$ – follow the distribution given in equation (11), thus ϕ cannot be exactly uniformly distributed. However, the deviations from uniformity are small.

The distribution of exiting points for both a cube and a slab are shown at the bottom panel of Figure 2. For this figure we assume that we observe photons emerging along the z direction and we record the x and y coordinates of their exit points (in units of the size of the cube). In the case of RT in a cube the distribution is pretty close to uniform. In the case of the slab, despite it being semi-infinite, for any practical purposes one can assume that all photons exit at most within $|x|(|y|) \leq 5$ (not shown in figure).

I want to thank A.V. Kravtsov for discussions and comments on the manuscript, and M. Dijkstra and N.Y. Gnedin for useful interaction. This work was supported through the Lyman Spitzer, Jr. Postdoctoral Fellowship at Princeton University and, in part, by the Kavli Institute for Cosmological Physics at The University of Chicago and by the National Science Foundation under grant NSF PHY 0114422.

REFERENCES

- Adams, T. F. 1972, ApJ, 174, 439
- Ahn, S., Lee, H., & Lee, H. M. 2002, ApJ, 567, 922
- Dijkstra, M., Haiman, Z., & Spaans, M. 2005, astro-ph/0510407
- Eddington, A. S. 1926, *The internal constitution of the stars* (London: Cambridge University Press)
- Harrington, J. P. 1973, MNRAS, 162, 43
- Neufeld, D. A. 1990, ApJ, 350, 216
- Norman, M. L. 2004, in *Adaptive Mesh Refinement - Theory and Applications*, Eds. T. Plewa, T. Linde and V. G. Weirs, Springer Lecture Notes in Computational Science and Engineering
- Phillips, K. C. & Meszaros, P. 1986, ApJ, 310, 284
- Stenflo, J. O. 1980, Astron. & Astrophys., 84, 68
- Tasitsiomi, A. 2005, astro-ph/0510347
- Unno, W. 1955, PASJ, 7, 81